Large-scale fabrication of plasmonic gold nanohole arrays for refractive index sensing at visible region

Ke Cheng, Shujie Wang, Zhonggang Cui, Qianqian Li, Shuxi Dai et al.

Related Articles

Dimensionality effects on the magnetization reversal in narrow FePt nanowires
Appl. Phys. Lett. 100, 252403 (2012)

Structural variation of hydrothermally synthesized KNbO3 nanowires
J. Appl. Phys. 111, 114314 (2012)

Long lifetime, high density single-crystal erbium compound nanowires as a high optical gain material
Appl. Phys. Lett. 100, 241905 (2012)

A polymer electrolyte with high luminous transmittance and low solar throughput: Polyethyleneimine-lithium bis(trifluoromethylsulfonyl) imide with In2O3:Sn nanocrystals
Appl. Phys. Lett. 100, 241902 (2012)

A new type of optical biosensor from DNA wrapped semiconductor graphene ribbons
J. Appl. Phys. 111, 114703 (2012)

Additional information on Appl. Phys. Lett.

Journal Homepage: http://apl.aip.org/

Journal Information: http://apl.aip.org/about/about_the_journal

Top downloads: http://apl.aip.org/features/most_downloaded

Information for Authors: http://apl.aip.org/authors
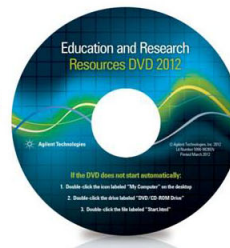
Large-scale fabrication of plasmonic gold nanohole arrays for refractive index sensing at visible region

Ke Cheng, Shujie Wang, Zhonggang Cui, Qianqian Li, Shuxi Dai, and Zuliang Du[a]

Key Laboratory for Special Functional Materials of Ministry of Education, Henan University, Kaifeng 475004, People's Republic of China

We present the design and fabrication of large-scale gold nanohole arrays based on the versatile nanosphere lithography technique. The gold nanohole arrays exhibit two surface plasmonic resonance related transmission peaks and show a sensitive response to refractive index. The working wavelength and sensitivity can be tuned by changing the hole diameter and hole depth. A sensitivity of 125 nm/refractive index unit is obtained in the visible region. Our quasi-infinite gold nanohole arrays film can serve as an optical enhancing component while also can serve as a transparent conductive electrode for the opto-electric devices. © *2012 American Institute of Physics.* [http://dx.doi.org/10.1063/1.4728987]

Since Ebbesen and co-workers reported that the light transmission through a periodic arrays of subwavelength holes in an optically thick metallic film can be several orders of magnitude higher than that described in the classical Bethe's theory in 1998,[1] plasmonic metal nanostructures, ranging from isolated metal nanoparticles to precisely fabricated order metal arrays had been extensively investigated both for scientific interest and for practical applications.[2–6] Surface plasmon resonance (SPR) is generally proposed to explain the enhanced optical transmission (EOT) phenomenon observed on periodically arrayed nanoholes. SPR is collective charge oscillations that are produced by the resonant interaction between incident light and free electrons at the interface between a metal and a dielectric.[7–11] Due to their interfacial nature, SPR is very sensitive to the surface chemistry and the refractive index of the environment surrounding. The adsorption of molecules to a metal surface significantly changes the oscillation of SP, which can modulate the light output. The modulation can be monitored either the intensity or the spectrum shift by the transmission at normal incident. Such characteristic provided the basis of SPR-based chemo- and biosensors.[12] The greatest attraction of nanoplasmonic sensing is it does not require extrinsic fluorescent or radioactive labeling (i.e., "label-free"), which is traditionally performed on prisms (Kretschmann geometry) or grating couplers.[13] De Leebeeck *et al.* had showed the feasibility of using periodic nanoholes for biosensing and observed a spectral shift after the immobilization of molecules.[14]

Based on recent advances in fabrication techniques such as electron beam lithography (EBL), focused ion beam (FIB) lithography, and phase-shifting lithography (PSL), a large class of SPR-based metal nanostructures such as nanodisks, nanoholes, bowtie antennas, and nanorings have been fabricated exhibiting high sensitivity based on localized surface plasmon resonance (LSPR) or coupled plasmonic resonance.[15–18] Among them, nanohole arrays can provide a smaller foot-print, denser integration, increased potential for

multiplexing and simplified collinear optical detection in which analyte binding is determined directly from light that is transmitted through the holes.[19,20] However, ordered metal nanostructures have been only fabricated with a finite area (always tens to hundreds of μm^2) using the slow and expensive "top-down" fabrication methods mentioned above.[21–23] This would result in a spectrum change due to the significant contribution from edges. In addition, the SPR not only depends on the material's dielectric properties but also the nanohole arrays geometry, hole diameter, and film thickness.[24] Understanding the effect of these factors is crucial for probing the underlying physics mechanisms for both the intensity and spectral nature of transmitted light through the nanohole arrays, which is still open for debate.[25] Moreover, developing a versatile and large-scale fabrication technique of nanohole arrays itself is crucial for its real devices applications. Therefore, a large-area fabrication of the nanohole arrays at fast rate and good reproducibility with controllable hole diameter, and hole depth is highly desired.

In this work, we reported the design and fabrication of a SPR-based nanohole arrays by modified nanosphere lithography (NSL) technique, which is a well-known, low-cost, and high-throughput method.[26,27] Furthermore, the NSL process allows for the fabrication of nanohole arrays with the advantage of hole size modification with reactive ion etch (RIE) while the periodicity of the nanohole array is fixed strictly due to the nature of NSL. This is valuable for understanding the various mechanisms involved in enhanced transmission of light through nanohole arrays.

The monolayer polystyrene (PS) masks were fabricated on the quartz glass by the modified floating-transferring technique.[26] Using this, we can obtain a large-scale 2D close-packed colloidal crystal mask on the quartz glass substrate. The sphere diameter we used here was about 330 nm. After the fabrication of PS masks, the diameters of the PS spheres were tailored by RIE treatments. For different gold nanohole diameters, the etching time of 10, 15, and 20 s was performed. Thereafter, the gold film (purity > 99.999%) was sputtered on the etched PS sphere masks by pulsed magnetron sputtering for 30 s. The gold cannot enter the area shadowed by the PS

[a]Author to whom correspondence should be addressed. Electronic mail: zld@henu.edu.cn.
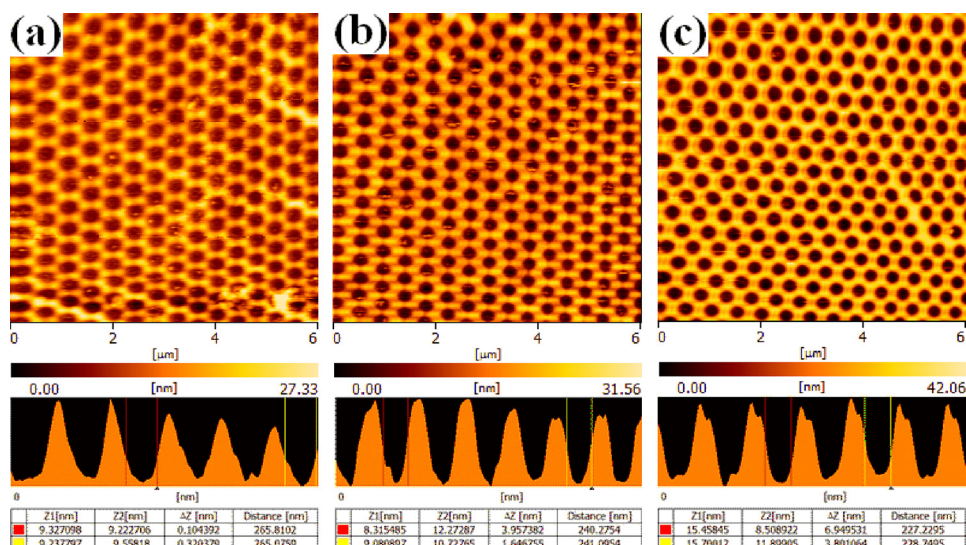
FIG. 1. The morphology and hole diameter analysis of Au nanohole arrays etched at different time: (a) 10 s; (b) 15 s; and (c) 20 s.

spheres which leaves a nanohole at the shadow position when the PS sphere was removed. For comparison, a sputtering time of 50 s was performed on another 15 s etched PS mask to increase the Au film thickness (hole depth). Finally, the PS spheres were thoroughly removed by dissolution in chloroform with a gentle ultrasonic bath for 1 min.

The nanohole arrays morphologies and analysis for different etching time were shown in Figure 1. We could see that the gold nanohole formed but relatively thin for the 10 s etching, which was not continuous in some locations because no sufficient gold could infiltrate the PS spheres voids. The Au wall thickness increased with the etching time increased to 15 s. Finally, a perfect continuous Au nanohole arrays with a large area (as shown in inset in Figure 2, the area just limited by the substrate used) obtained as shown in Figure 1(c). Nanohole diameters of the arrays were characterized via atomic force microscopy morphologies analysis to be 265, 240, and 227 nm, respectively, for the 10, 15, and 20 s etching times as shown in Figure 1. We can see that the periodicity (~330 nm in our case, determined by the PS sphere diameter used) fixed strictly for all the nanohole arrays due to the nature of NSL. The composition of the pure gold film

and 15 s etched nanohole arrays film were characterized by x-ray diffraction (XRD) as shown in Figure 2.

Figure 3 showed the transmission spectra for the nanohole arrays with different hole diameters. The transmission spectra obtained directly from the nanohole arrays in air at normal incidence, which was recorded over a wavelength range from 400 to 1100 nm. The transmission peak around 510 nm presented in both pure and nanohole arrays gold films could be assigned to the transitions from the conduction band to the d-energy band.[28] It should be noted that there is a slight blue-shift for the transmission peak around 510 nm with the hole diameter decrease for the nanohole arrays. Since the transition peak cannot move with the change of nanohole geometry,[29] the trasmission peak around 510 nm for the nanohole arrays film could be assigned to the co-actions of transitions from the conduction band to the d-energy band and plasmonic effects. Such conclusion could also be confirmed by the work of Sharpe *et al.*[15] The first $\lambda_{max}(1, 1)$ (associate with the air-gold nanohole interface) SPR peak they obtained at 737 nm using an Au nanohole arrays with a periodicity of 520 nm. As we know, the approximate position of the SPR peaks can be determined by the equation:[30]
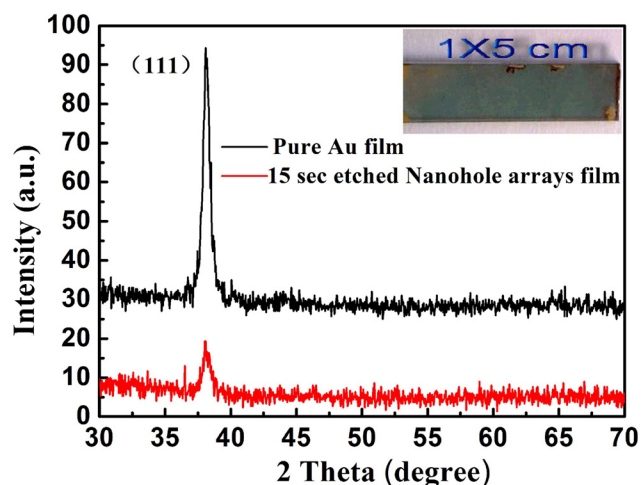
FIG. 2. X-ray diffraction spectrum of pure Au film and nanohole arrays film with 15 s etching. Inset is the photography of large-scale gold nanohole arrays.
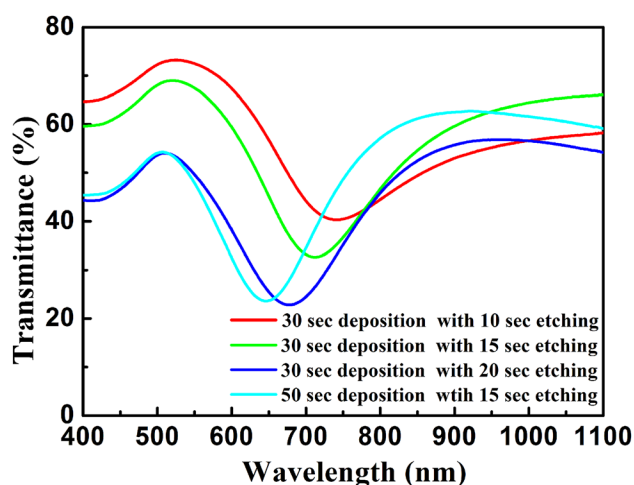
FIG. 3. Optical transmission spectrum of the nanohole arrays with different hole diameters and hole depth.

$$\lambda_{\max}(i,j) = \frac{P}{\sqrt{(i^2+j^2)}}\sqrt{\frac{\varepsilon_1\varepsilon_2}{(\varepsilon_1+\varepsilon_2)}}, \qquad (1)$$

where P is the periodicity of the network of the arrays, ε_1 and ε_2 are the dielectric constants of the metal and the dielectric material in contact with the metal respectively, and i, j are the scattering orders of the arrays. From Eq. (1), we can see that the $\lambda_{\max}$ proportionate to the periodicity. In our case, the periodicity was about 330 nm, which is lower than that of Sharpe's *et al*. Therefore, the first $\lambda_{\max}(1,1)$ SPR peak blue shifted and made a superposition with the 510 nm transition peak of the gold film itself.

The maximum broad transmission around 800–1100 nm occurs through the excitation of SP waves in the nanohole arrays, which acts as a two-dimensional diffraction grating that converts incident photons into SP waves. The basic mechanism involved in the enhanced transmission process is (1) photons couple to SPs on the incident side of a nanohole arrays film, (2) the SPs propagate through the nanoholes to the opposite side, and (3) the SPs are converted back to photons and re-radiated.[9] We observed that the second (1, 0) (associate with the gold nanohole-quartz glass interface) peak shifted from 850 nm to over 1100 nm. The peak values could not be quantified exactly due to the wavelength beyond the efficient range of our spectrometer. However, a minimum transmission at 620–720 nm could be observed clearly, which was so-called Wood anomaly.[31] The film thickness is below 50 nm for our case, which can be approximately obtained from the hole diameter analysis shown in Figure 1. Such thickness indicate that light can transmit directly through the gold film and interfere with the re-emitted plasmon resonance light, which results in a transmission minimum as we observed. Similar transmission minimum phenomena had also been reported for nanohole films with a thickness close to the skin depth.[32]

The transmission minimum blue-shifted from 737 to 677 nm as the hole diameter decreased from 265 to 227 nm as observed in Figure 3. When we increased the hole depth by increasing the gold deposition time to 50 s, a further blue-shifted to 646 nm could be observed. In our case, the periodicity and dielectric environment of all the nanohole arrays films were the same. This indicated that a blue-shift occurred when the aspect ratio of nanohole diameter to nanohole depth was decreased. However, Eq. (1) does not predict such an effect. Therefore, a more complicated equation should be established to predict the SPR peak position exactly. The transmission minimum peak of the thicker film became sharper slightly than that of the thinner one. The full width at half-maximum (FWHM) was 126.8 nm and 163.1 nm for the thicker film and the thinner film with a 20 s etching time, respectively, which was obtained from Figure 3. Such phenomenon was also observed by Ebbesen's group.[33] That is, the ratio of the metal film thickness (T) and hole diameter (D) T/D is more close to 1, a sharper maximum transmission will be obtained, which is very important for the sensitive detection of small changes in the refractive index of the surroundings.[34]

The refractive index sensing experiments of 15 s etched nanohole arrays were performed simply by immersing the samples in index matching liquids with different refractive indices from 1 (air), 1.36 (ethanol), to 1.44 (chloroform). We observed that the spectra red-shifted with the increased refractive index, which was in agreement with established theory of light transmission through nanoholes.[35] For comparison, the transmission spectrum of a pure gold film was also characterized at the same conditions. Only a single transmission peak at 510 nm without any shift with the change of dielectric surroundings could be observed as shown in the inset of Figure 4. This was a direct evidence for our conclusion that transmission peak around 510 nm observed in Figure 3 is a co-actions of transition and plasmonic effects. The refractive index sensitivity S can be defined as: $S = \Delta\lambda/(n_{med} - n_{air})$. The $\Delta\lambda$ was measured from the wavelength shift of transmission minimum with the variation of the refractive index. A maximum sensitivity about 125 nm/refractive index unit (RIU) could be obtained, which was lower than that of previously reported.[15] The lower sensitivity is due to the visible light we used here as the sensing wavelength, which causes less shift of the spectra feature than that of infrared light.[36] However, the advantage using visible region sensing is that it can prevent potential near-infrared adsorption of water and many biological species effectively.[36] On the other hand, Pang *et al*. had reported that the sensitivity depend on the periodicity of the nanohole arrays.[37] Therefore, using a appropriate diameter of PS sphere would improve the sensitivity of our nanohole arrays.

In conclusion, a simple and massive nanofabrication technique is reported to produce large area gold nanohole arrays based on the NSL. The working wavelength and sensitivity can be tuned by changing the hole diameter and hole depth. The gold nanohole arrays exhibit two SPR related transmission peaks and show a sensitive response to refractive index. A sensitivity of 125 nm/RIU is obtained at the visible region. More importantly, our large-area continuous gold nanohole arrays film can be served as an optical enhancing component in photo-electric devices while also served as a carrier extracting electrode. It is difficult for other metal nanoparticles or metal nanostructrues to perform dual optical and electrical
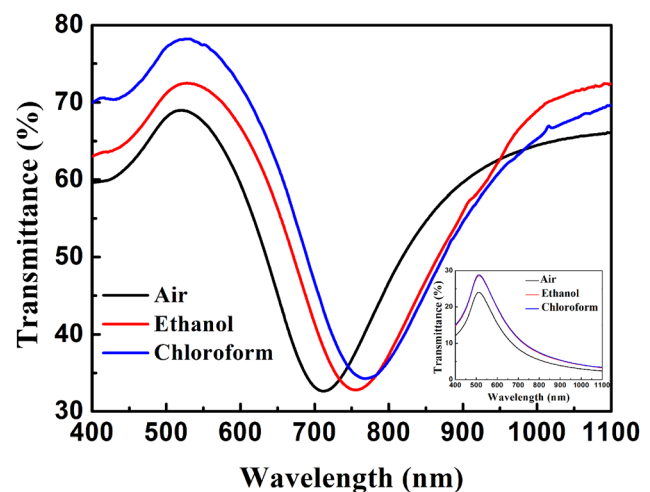
FIG. 4. Sequence of transmission spectra through the 15 s etched nanohole arrays as the refractive index increases from 1 to 1.44. Inset is the transmission spectra of pure gold film at the same conditions.

roles since they are limited by the finite fabrication area and isolated nature without electrically connecting.

[1] T. W. Ebbesen, H. J. Lezec, H. F. Ghaemi, T. Thio, and P. A. Wolff, Nature (London) **391**, 667 (1998).

[2] B. W. Wang, M. A. Dundar, R. Notzel, F. Karouta, S. He, and R. W. V. D. Heijden, Appl. Phys. Lett. **97**, 151105 (2010).

[3] C. Y. Tsai, S. P. Lu, J. W. Lin, and P. T. Lee, Appl. Phys. Lett. **98**, 153108 (2011).

[4] R. Gordon, M. Hughes, B. Leathem, K. L. Kavanagh, and A. G. Brolo, Nano Lett. **5**, 1243 (2005).

[5] I. M. Pryce, Y. A. Kelaita, K. Aydin, and H. A. Atwater, ACS Nano **5**, 8167 (2011).

[6] J. Henzie, M. H. Lee, and T. W. Odom, Nat. Nanotechnol. **2**, 549 (2007).

[7] S. Wu, J. Q. Liu, L. Zhou, Q. J. Wang, Y. Zhang, G. D. Wang, and Y. Y. Zhu, Appl. Phys. Lett. **99**, 141104 (2011).

[8] H. Im, N. C. Lindquist, A. Lesuffleur, and S. H. Oh, ACS Nano **4**, 947 (2010).

[9] T. H. Reilly, R. C. Tenent, T. M. Barnes, K. L. Rowlen, and J. V. D. Lagemaat, ACS Nano **4**, 615 (2010).

[10] A. G. Brolo, S. C. Kwok, M. G. Moffitt, R. Grodon, J. Riordon, and K. L. Kavanagh, J. Am. Chem. Soc. **127**, 14936 (2005).

[11] J. Maria, T. T. Truong, J. M. Yao, T. W. Lee, R. G. Nuzzo, S. Leyffer, S. K. Gray, and J. A. Rogers, J. Phys. Chem. C **113**, 10493 (2009).

[12] P. F. Guo, S. Wu, Q. J. Ren, J. Lu, Z. H. Chen, S. J. Xiao, and Y. Y. Zhu, J. Phys. Chem. Lett. **1**, 315 (2010).

[13] H. K. Hunt and A. M. Armani, Nanoscale **2**, 1544 (2010).

[14] A. D. Leebeeck, L. K. S. Kumar, V. D. Lange, D. Sinton, R. Gordon, and A. G. Brolo, Anal. Chem. **79**, 4094 (2007).

[15] J. C. Sharpe, J. S. Mitchell, L. Lin, N. Sedoglavich, and R. J. Blaikie, Anal. Chem. **80**, 2244 (2008).

[16] F. J. Rodriguez-Fortuno, M. Martinez-Marco, B. Tomas-Navarro, R. Ortuno, J. Marti, A. Matinez, and P. J. Rodriguez-Canto, Appl. Phys. Lett. **98**, 133118 (2011).

[17] M. D. He, Z. Q. Gong, S. Li, Y. F. Luo, and J. Q. Liu, J. Appl. Phys. **108**, 093520 (2010).

[18] H. Oshima, H. Kikuchi, H. Nakao, K. I. Itoh, and T. Kamimura, Appl. Phys. Lett. **91**, 022508 (2007).

[19] H. W. Gao, J. Henzie, and T. W. Odom, Nano Lett. **6**, 2104 (2006).

[20] C. Escobedo, A. G. Brolo, R. Gordon, and D. Sinton, Anal. Chem. **82**, 10015 (2010).

[21] S. A. Kim, K. M. Byun, K. Kim, S. M. Jang, K. Ma, Y. Oh, D. Kim, S. G. Kim, M. L. Shuler, and S. J. Kim, Nanotechnology **21**, 355503 (2010).

[22] N. C. Lindquist, A. Lesuffleur, and S. H. Oh, Appl. Phys. Lett. **91**, 253105 (2007).

[23] L. Y. Wu, B. M. Ross, and L. P. Lee, Nano Lett. **9**, 1956 (2009).

[24] J. C. Yang, H. W. Gao, J. Y. Sun, W. Zhou, M. H. Lee, and T. W. Odom, Nano Lett. **10**, 3173 (2010).

[25] T. H. Park, N. Mirin, J. B. Lassiter, C. L. Nehl, N. J. Hales, and P. Nordlander, ACS Nano **2**, 25 (2008).

[26] Q. F. Yan, L. K. The, Q. Shao, C. C. Wong, and Y. M. Chiang, Langmuir **24**, 1796 (2008).

[27] S. K. Yang and Y. Lei, Nanoscale **3**, 2768 (2011).

[28] A. V. Kabashin, P. Evans, S. Pastkovsky, W. Hendren, G. A. Wurtz, R. Atkinson, R. Pollard, V. A. Podolskiy, and A. V. Zayats, Nature Mater. **8**, 867 (2009).

[29] J. H. Kim and P. J. Moyer, Appl. Phys. Lett. **89**, 121106 (2006).

[30] A. Lesuffleur, H. Im, N. C. Lindquist, and S. H. Oh, Appl. Phys. Lett. **90**, 243110 (2007).

[31] S. Wu, P. F. Guo, W. X. Huang, S. J. Xiao, and Y. Y. Zhu, J. Phys. Chem. C **115**, 15205 (2011).

[32] T. Sannomiya, O. Scholder, K. Jefimovs, C. Hafner, and A. B. Dahlin, Small **7**, 1653 (2011).

[33] J. Ji, J. G. O'Connell, D. J. D. Carter, and D. N. Larson, Anal. Chem. **80**, 2491 (2008).

[34] P. Offermans, M. C. Schaafsma, S. R. K. Rodriguez, Y. C. Zhang, M. Cergo-Calama, S. H. Brongersma, and J. G. Rivas, ACS Nano **5**, 5151 (2011).

[35] Q. M. Yu, P. Guan, D. Qin, G. Golden, and P. M. Wallace, Nano Lett. **8**, 1923 (2008).

[36] J. C. Yang, J. Ji, J. M. Hogle, and D. N. Larson, Nano Lett. **8**, 2718 (2008).

[37] L. Pang, G. M. Hwang, B. Slutsky, and Y. Fainman, Appl. Phys. Lett. **91**, 123112 (2007).